

AD-A070 768

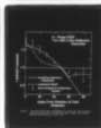
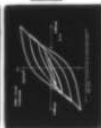
NATIONAL BUREAU OF STANDARDS WASHINGTON DC POLYMER --ETC F/G 20/3  
FERROELECTRIC POLARIZATION IN POLYMERS.(U)  
JUN 79 M G BROADHURST, G T DAVIS

UNCLASSIFIED

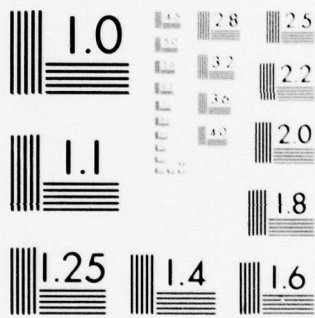
TR-13

N00014-79-C-0012  
NL

1 OF 1  
AD  
A070768



END  
DATE  
FILMED  
8-79  
DDC



MICROCOPY RESOLUTION TEST CHART  
NATIONAL BUREAU OF STANDARDS-1963-A

# LEVEL

(12)

OFFICE OF NAVAL RESEARCH

Contract ~~NO0014-79-7-0012~~ NO0014-79-C-0012

Task No. 12139

TECHNICAL REPORT NO. 13

FERROELECTRIC POLARIZATION IN POLYMERS

by

M. G. Broadhurst and G. T. Davis

Prepared for Publication

in the

Proceedings from Conference on Electrical Insulation  
and Dielectric Phenomena

410 345  
National Bureau of Standards  
Polymer Science & Standards Division  
Washington, D.C. 20234

June, 1979

Reproduction in whole or in part is permitted for  
any purpose of the United States Government

This document has been approved for public release  
and sale; its distribution is unlimited.

DDC  
RECEIVED  
JUL 2 1979  
RECEIVED

ADA070768

DDC FILE COPY

REPORT DOCUMENTATION PAGE		READ INSTRUCTIONS BEFORE COMPLETING FORM
1. REPORT NUMBER Technical Report # 13	2. GOVT ACCESSION NO.	3. RECIPIENT'S CATALOG NUMBER
4. TITLE (and Subtitle) <u>FERROELECTRIC POLARIZATION IN POLYMERS,</u>	5. TYPE OF REPORT & PERIOD COVERED <u>Technical Report # 13</u>	
7. AUTHOR(s) <u>Martin G. Broadhurst and G. Thomas Davis</u>	6. CONTRACT OR GRANT NUMBER(s) <u>N00014-79-X-0012</u>	
9. PERFORMING ORGANIZATION NAME AND ADDRESS National Bureau of Standards Polymer Science and Standards Division Washington, D.C. 20234	10. PROGRAM ELEMENT, PROJECT, TASK AREA & WORK UNIT NUMBERS  Task No. 12139	
11. CONTROLLING OFFICE NAME AND ADDRESS Office of Naval Research Chemistry Program Arlington, VA 22217	12. REPORT DATE <u>June 1979</u>	
14. MONITORING AGENCY NAME & ADDRESS (if different from Controlling Office) <u>TR-13</u> <u>13</u> <u>19 p.</u>	13. NUMBER OF PAGES 13	
	15. SECURITY CLASS. (of this report) Unclassified	
	15a. DECLASSIFICATION/DOWNGRADING SCHEDULE	
16. DISTRIBUTION STATEMENT (of this Report)  Distribution Statements on Technical Documents <div style="border: 1px solid black; padding: 5px; display: inline-block;">This document has been approved for public release and sale; its distribution is unlimited.</div>		
17. DISTRIBUTION STATEMENT (of the abstract entered in Block 20, if different from Report) <u>N00014-79-X-0012</u>		
18. SUPPLEMENTARY NOTES To be published in Proceedings from Conference on Electrical Insulation and Dielectric Phenomena - 1979.		
19. KEY WORDS (Continue on reverse side if necessary and identify by block number) Cooperative Rotations; ferroelectric; hysteresis ; infra red transmission; piezoelectric; polarization; polyvinylidene fluoride; x-ray pole figures.		
20. ABSTRACT (Continue on reverse side if necessary and identify by block number) A cooperative model has been developed to describe ferroelectric polarization in polyvinylidene fluoride (PVDF). The molecular dipoles within the crystal are assumed to have two or more orientations available to them and the lattice energy of a given orientational site is assumed to be proportional to the fraction of molecules having that orientation. An analytical solution is given for the 2-site model which predicts polarization hysteresis typical of ferroelectrics. However, a more complex 6-site model, which can be analysed		

Block 20 - continued

numerically, is needed to account for observed infra red hysteresis data and electric-field-induced x-ray structural changes which have been reported for PVDF. Although the model is simple, rather complex behavior is observed including a gradual increase or decrease in the remnant polarization with number of cycles of electric field application. Though the agreements with various experimental data are good an obvious need to include kinetic effects in the model is indicated.

Accession For	
NTIS GMA&I	<input checked="checked" type="checkbox"/>
DDC TAB	<input type="checkbox"/>
Unannounced	<input type="checkbox"/>
Justification	
By _____	
Distribution/ _____	
Availability _____	
Dist	Avail and or special
A	



## FERROELECTRIC POLARIZATION IN POLYMERS

M. G. Broadhurst and G. T. Davis  
National Bureau of Standards  
Washington, D.C. 20234

### INTRODUCTION

Previous work has shown that a model of oriented dipoles accounts quite well for observed piezoelectric and pyroelectric behavior of amorphous<sup>1</sup> and semicrystalline<sup>2</sup> polymers. The process whereby the dipoles become oriented is the subject of this paper. Here we summarize a model and calculated results for ferroelectric reorientation of molecular dipoles in the all-trans polar crystal phase ( $\beta$  phase or Form I) of polyvinylidene fluoride. By ferroelectric we mean a material with polar crystals where the polarization direction can be reversed with an applied electric field.

In the model, the orientations of molecular dipoles depend on the electric field and the history of the field application. The quantities  $\langle \cos \theta \rangle$ ,  $\langle \cos^2 \theta \rangle$ , and  $f(\theta)$  can be calculated where  $\theta$  is the angle between a dipole and the applied field,  $f(\theta)$  is the fraction of dipoles at angle  $\theta$  and the brackets  $\langle \rangle$  indicate a spacial average. The experimental physical quantities of interest for comparison with the model are polarization (a measure of  $\langle \cos \theta \rangle$ ), infra red transmission intensity<sup>3,4</sup> (a measure of  $\langle \cos^2 \theta \rangle$ ) and x-ray pole figure data<sup>5</sup> (a measure of  $f(\theta)$ ). Since only one adjustable parameter is used in the model, these various comparisons permit an unusually thorough evaluation of the strengths and weaknesses of the model.

### THE MODEL

Polyvinylidene fluoride (PVDF) is a linear molecule with a carbon backbone. In its crystalline forms the molecule has a large moment normal to the chain.

In the  $\beta$  crystal phase the unit cell is polar and the crystals form lamellae typically 10 nm thick with the molecular segments nearly normal to the large crystal surfaces.<sup>2</sup> The molecular segments which traverse the crystal lamellae are interconnected through the intercrystalline amorphous regions (See Fig. 1) either by tight folds at the lamellar surface or by longer irregular molecular segments. As demonstrated in the data referenced later in this paper, the segments in the crystal can rotate as rigid rods or by a propagating twist mechanism about their chain axis, giving a reorientation of the crystal moment. The shape of the curve relating potential energy to angle for individual chain rotation is not known, but following Kepler and Anderson's observation that the near-hexagonal unit cell cross section will permit a six-fold degeneracy in the orientation of the crystal,<sup>5</sup> we assume equivalent potential energy minima, 60 degrees apart as shown in Fig. 2. The potential energy of an orientation  $\theta_i$  relative to a base line is  $U_i$  and the fraction of segments having that orientation is  $f_i$ . We use the first order, mean field cooperativity assumption<sup>6,7</sup> that  $U_i = -U_0 f_i$  where  $U_0$  is the energy difference between a filled and empty site. This assumption describes the desired feature that if most segments have a given orientation then that orientation is the preferred one (having the lowest energy). The lattice energy of the crystal is given by  $\sum U_i f_i = -U_0 \sum f_i^2$ , the dipole-field interaction energy is given by  $-m_0 E \sum f_i \cos \theta_i$  (where the field is assumed to be at 0 degrees), and the entropy is given by  $-k \sum f_i \ln f_i$ . We do not include dipole-dipole interactions. The Helmholtz free energy is

$$(A_i - A_0) = -U_0 \sum f_i^2 - m_0 E \sum f_i \cos \theta_i + kT \sum f_i \ln f_i \quad (1)$$

We can minimize the free energy including the constraint that  $\sum f_i = 1$  by using a Lagrange multiplier technique. That is, we solve the equations,

$$\partial(A_i - A_0) / \partial f_j - \lambda \partial(\sum f_i) / \partial f_j = 0. \quad (2)$$

The result is a set of 6 equations

$$-2U_0 f_i - m_0 E \cos \theta_i + kT(1 + \ln f_i) - \lambda = 0 \quad (3)$$

We can solve the simple 2 site case analytically<sup>8</sup> but this 6 site example must be solved numerically as detailed elsewhere.<sup>9</sup>

## RESULTS

The result of the calculation is that at  $E = 0$  for  $U_0/kT > 2.0118$  (an unusual type of Curie point for this model), the 6-fold-degenerate lowest energy solution is for one site to be heavily populated and the remaining five sites to have lesser (but equal to each other) populations. At  $|E| > 0$ , the degeneracy is removed and depending on  $E$  and the angle between  $E$  and a preferred site, a particular distribution may become unstable and a new distribution form resulting in a change in the magnitude and direction of the crystal moment. The assumed mode of redistribution of orientations is somewhat arbitrary but the one giving results closest to experiment assumes that once a site  $i$  is unstable, the probability that, of the remaining stable sites, site  $j$  will be favored is proportional to  $\exp(m_0 E \cos \theta_j / kT)$ . This assumption is not to be confused with the equilibrium assumption of Kepler and Anderson<sup>5</sup> that the population of site  $j$  will be proportional to this term. In our case the orientations are not at equilibrium and are highly dependent on the initial distribution of orientations and history of electric field application.

The numerical calculation is done by varying  $m_0 E / kT$  in equation 3 (after dividing by  $kT$ ) by small increments, recomputing  $f_i$  and if a given solution is unstable, redistributing the  $f_i$  as described above. We assumed an initial distribution of crystals such that the crystal moments and applied field are in the plane of the crystal lamellae and the moments are equally distributed every 10 degrees from 0 to 350 degrees. From the record of  $f_i$  versus  $E$  we calculate  $\langle \cos \theta \rangle$ ,  $\langle \cos^2 \theta \rangle$  and the fraction of reflecting crystal planes at



angle  $\theta_i$  as a function of field and history. To compare  $m_0 E/kT$  to the applied field we assume a molecular segment in the crystal is 10 nm long. Such a segment contains 40 repeat units of  $6.9 \times 10^{-30}$  Cm vacuum moment each. The reaction field (in the spherical approximation) enhances this moment by  $(\epsilon_c + 2)/3 \approx 5/3$  giving a total segment moment of  $4.6 \times 10^{-28}$  Cm. Thus, a 1 MV/cm field at room temperature gives  $m_0 E/kT = 11$ . This value is well above the range of linear dielectric response typically encountered with molecular dipoles. We used a lattice energy of  $U_0/kT = 3$  for our calculations which gives a critical field (for which the first crystals switch) of about 1 MV/cm. Remembering the  $U_0$  is the energy difference between an empty and filled site, we see that the dipole-field energy can be much greater than the crystal energies. Reducing  $U_0/kT$  to 2.5 reduces the critical field by half but as a function of reduced field,  $E/E$  (critical), the calculations are insensitive to  $U_0/kT$ . For simplicity, we have ignored kinetic effects in the calculations even though they are inherent in the model. For example, thermodynamic fluctuations will allow a crystal to switch to a new preferred orientation at fields below the critical value and all redistributions of dipoles involve rotations which encounter local energy barriers - a process which takes time.

#### COMPARISON WITH EXPERIMENT

The calculated polarization as a function of electric field through  $1\frac{1}{2}$  cycles is shown in Figure 3. Experimental curves obtained by cycling the field at a constant rate of change<sup>10</sup> are shown in Figure 4. Both the observed critical switching field and degree of polarization (as a fraction of the total possible polarization) are satisfactorily mimicked by the calculated curve. The quantity  $m_0 E/kT = 11$  corresponds to  $E = 1$  MV/cm for 10 nm thick crystals and for these mixed phase samples (30%  $\alpha$  crystals, 30%  $\beta$  crystals and 40% amorphous phase) the maximum polarization will be about  $10 \mu\text{C}/\text{cm}^2$ . To account for the reversible permittivity of the amorphous phase we have added a relative permittivity of 15 to the model which accounts for the slope in curves of Fig. 3 upon decreasing the field.

Figure 5 is a comparison between calculated  $\langle \cos^2\theta \rangle$  for the model and the measured hysteresis of the  $512\text{ cm}^{-1}$  IR absorption in PVDF<sup>3</sup>. This absorption is due to 3 phase crystal vibrations polarized parallel to the  $\text{CF}_2$  dipole moment. Random orientation of single axes rotators with the axes in the plane of the film corresponds to  $\langle \cos^2\theta \rangle = 0.5$  and 23% transmission. Complete alignment corresponds to  $\langle \cos^2\theta \rangle = 1.0$  and 40% transmission and these values are used to match the magnitudes of the ordinates. Thus the magnitudes and general positions of the two curves are very similar.

In Figure 6 we show calculated and observed x-ray pole figure results obtained at zero field after the material has been subjected to a polarization treatment. The abscissa refers to the angle between the bisector of the incident and diffracted x-ray beams and the normal to the PVDF film (or equivalently the direction of the poling field). The results from the present calculation (dashed curve) predict the correct magnitudes at zero and large angles and are less satisfactory than the equilibrium calculation<sup>5</sup> (solid line) at small angles.

While the above results support a conclusion that the essential features of the high field polarization in PVDF are described by a simple cooperative ferroelectric model, the curvature in the experimental hysteresis curves (Figs. 4 and 5) at zero fields is an obvious feature which has not been delineated in the present calculations.

#### ACKNOWLEDGEMENT

The authors are grateful for the partial support of this work provided by the Office of Naval Research.

## REFERENCES

1. F. I. Mopsik and M. G. Broadhurst, J. App. Phys. 46, 4204 (1975).
2. M. G. Broadhurst, G. T. Davis, J. E. McKinney and R. E. Collins, J. Appl. Phys. 49 4992 (1978).
3. D. Naegele and D. Y. Yoon, Appl. Phys. Lett. 33, 132 (1978).
4. E. Fukada, M. Date and T. Furekawa, Organ. Coatings Plast. Chem. 38, 262 (1978). (Preprints for ACS Meeting in Anaheim Calif., 1978).
5. R. G. Kepler and R. A. Anderson, J. Appl. Phys. 49, 1232 (1978).
6. W. L. Bragg and E. J. Williams, Proc. Ray. Soc. A 145, 699 (1934).
7. W. P. Mason, Phys. Rev. 72, 854 (1947).
8. M. G. Broadhurst and G. T. Davis, in Topics in Modern Physics - Electrets, G. M. Sessler, Ed. Springer-Verlag, in Press.
9. M. G. Broadhurst and G. T. Davis, intended for J. Appl. Phys.
10. Data of A. DeReggi and S. C. Roth, at NBS.



#### FIGURE CAPTIONS

- Figure 1. Structure of semicrystalline polyvinylidene fluoride showing lamellar crystals with molecular segments normal to the lamellae.
- Figure 2. Assumed potential energy of a single molecular segment rotating about its chain axis as a function of angle between its dipole moment and a direction fixed in the crystal. The fraction of all molecules in a crystal having orientation  $i$  is given by  $f_i$ .
- Figure 3. Calculated polarization hysteresis for the 6-site model assuming 10nm long molecular segments rotating about their long axis.
- Figure 4. Experimental polarization hysteresis for a sample cycled at increasingly higher fields. The maximum residual polarization (at zero field) is about  $10\mu\text{C}/\text{cm}^2$ .
- Figure 5. Experimental (Reference 3) and calculated infra red transmission hysteresis for a vibration polarized along the  $\text{CF}_2$  dipole in the  $\beta$  crystal phase.
- Figure 6. X-ray pole figure data from Reference 5 (error bars) and calculated results from the 6-site ferroelectric model (dashed line) and an equilibrium distribution (solid line).



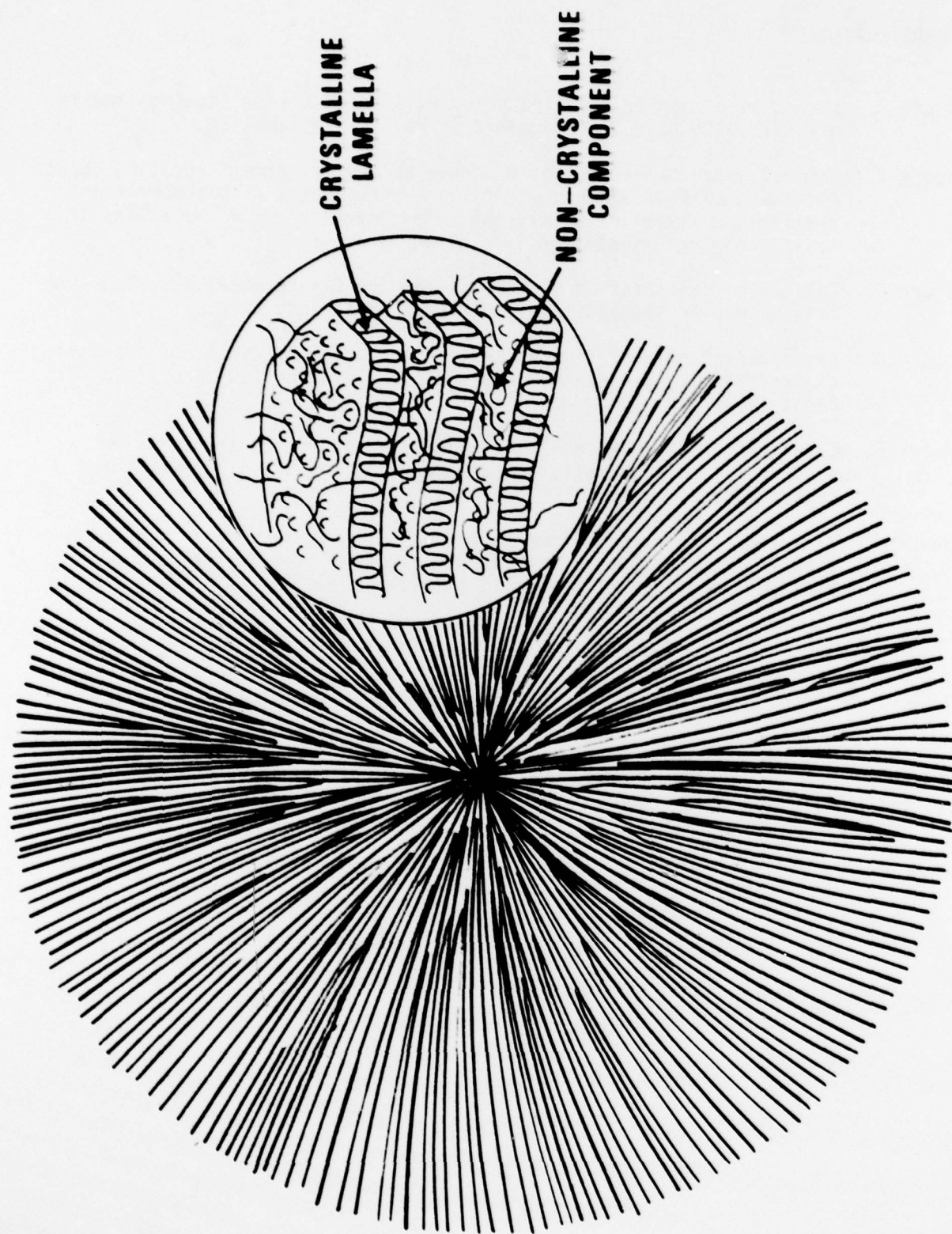


Figure 1. Structure of semicrystalline polyvinylidene fluoride showing lamellar crystals with molecular segments normal to the lamellae.

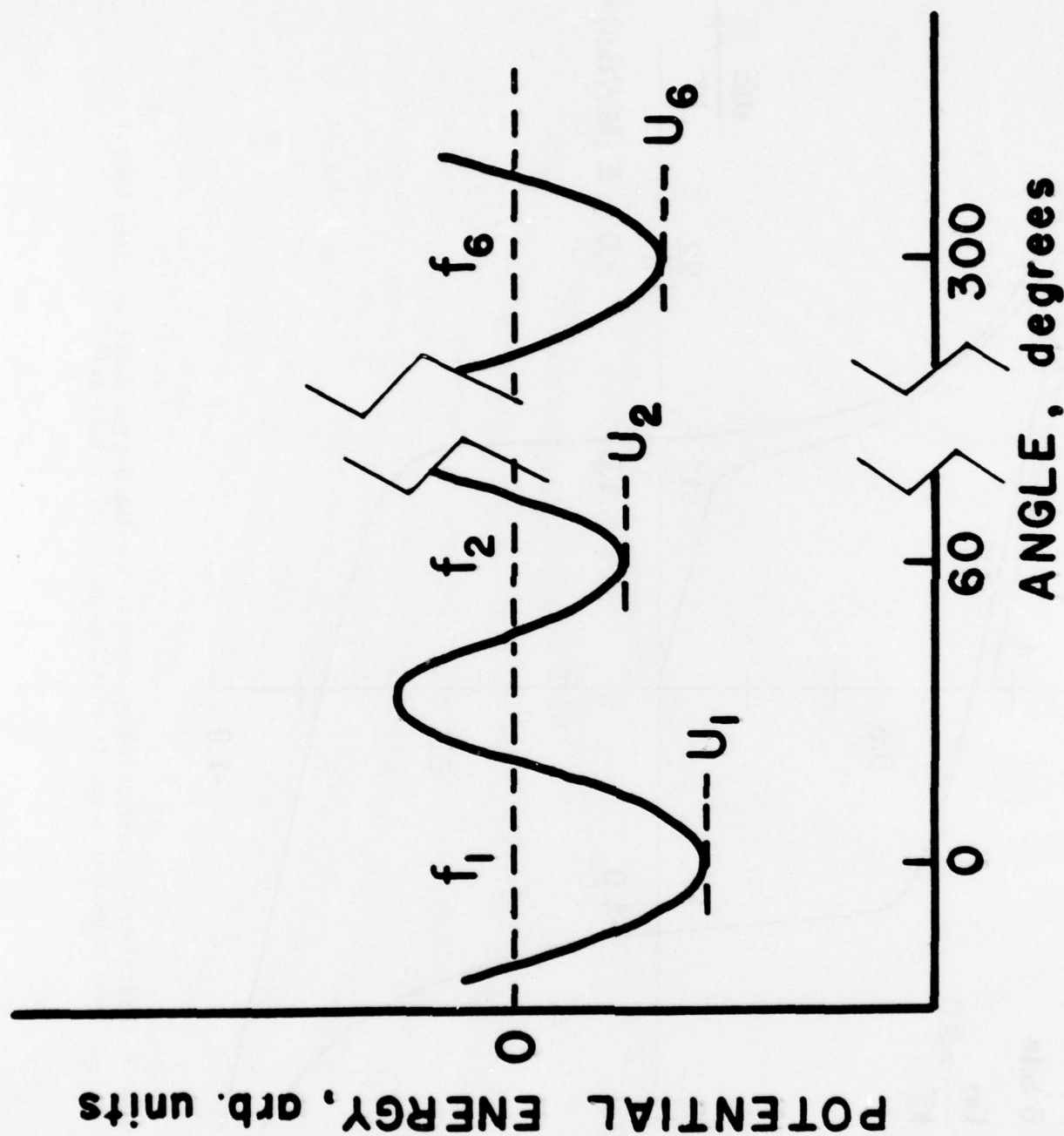


Figure 2. Assumed potential energy of a single molecular segment rotating about its chain axis as a function of angle between its dipole moment and the electric field direction. The fraction of all molecules in a crystal having orientation  $i$  is given by  $f_i$ .

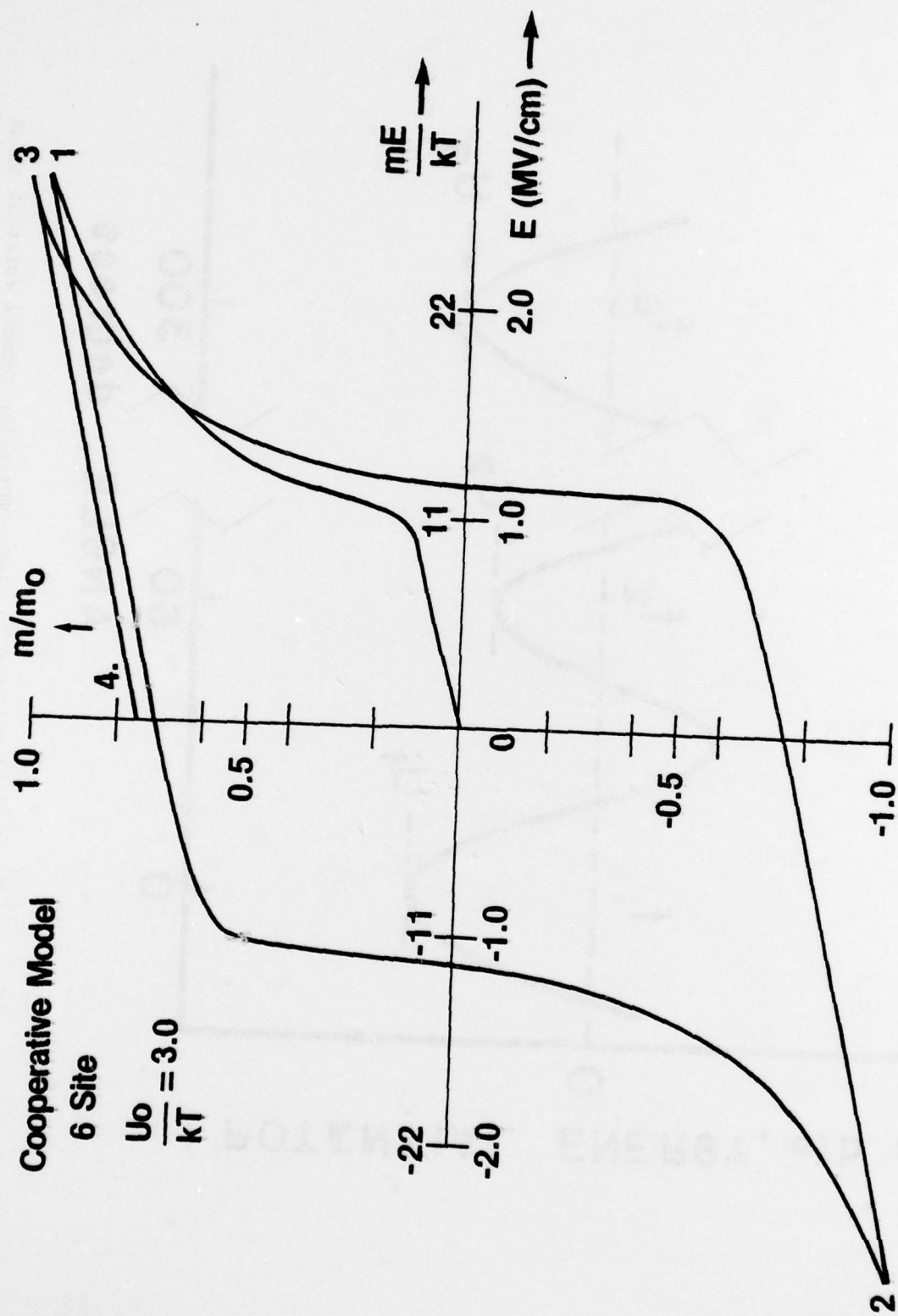


Figure 3. Calculated polarization hysteresis for the 6-site model assuming 10nm long molecular segments rotating about their long axis.

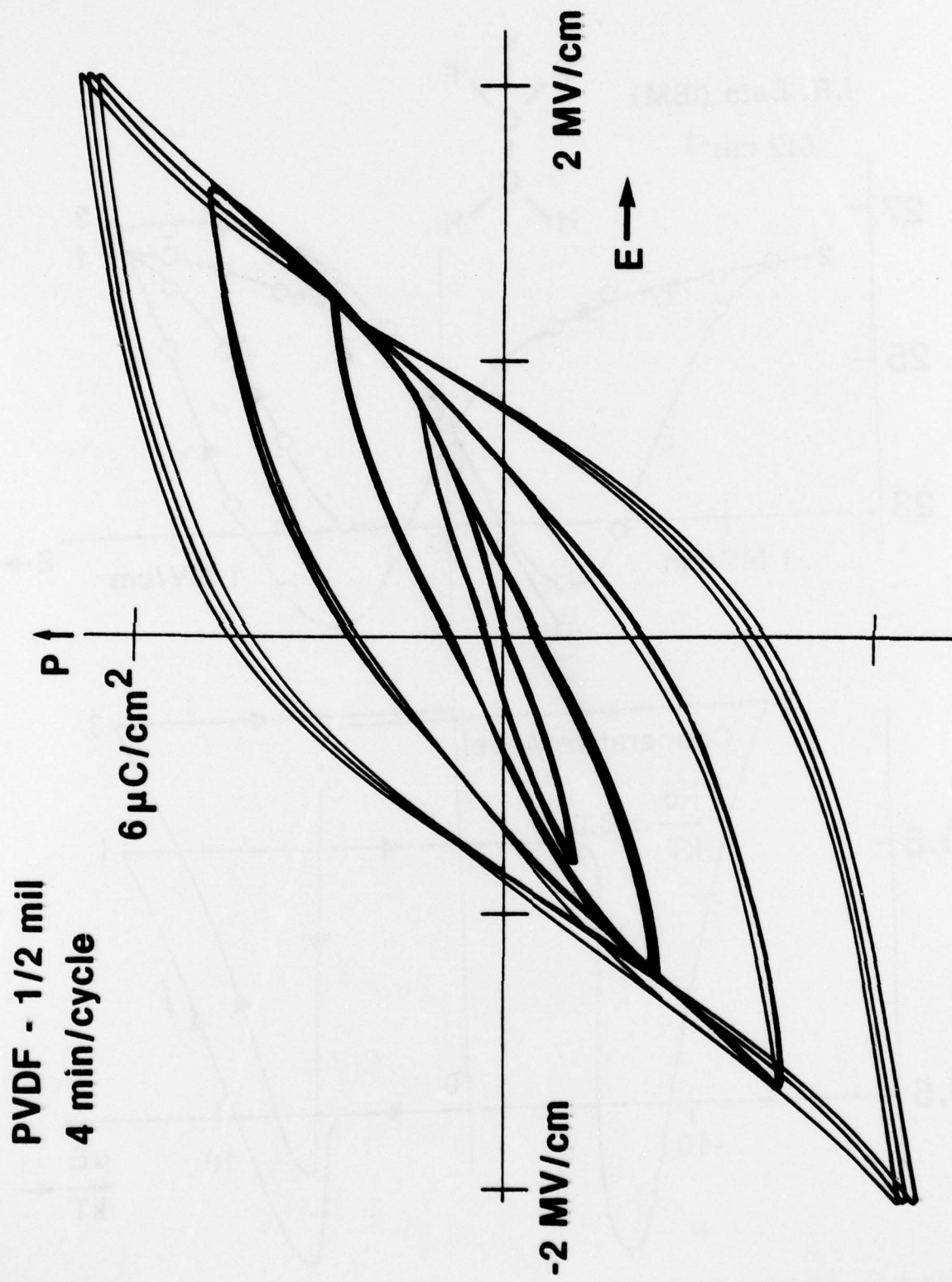


Figure 4. Experimental polarization hysteresis for a sample cycled at increasingly higher fields. The maximum residual polarization (at zero field) is about  $10 \mu\text{C}/\text{cm}^2$ .



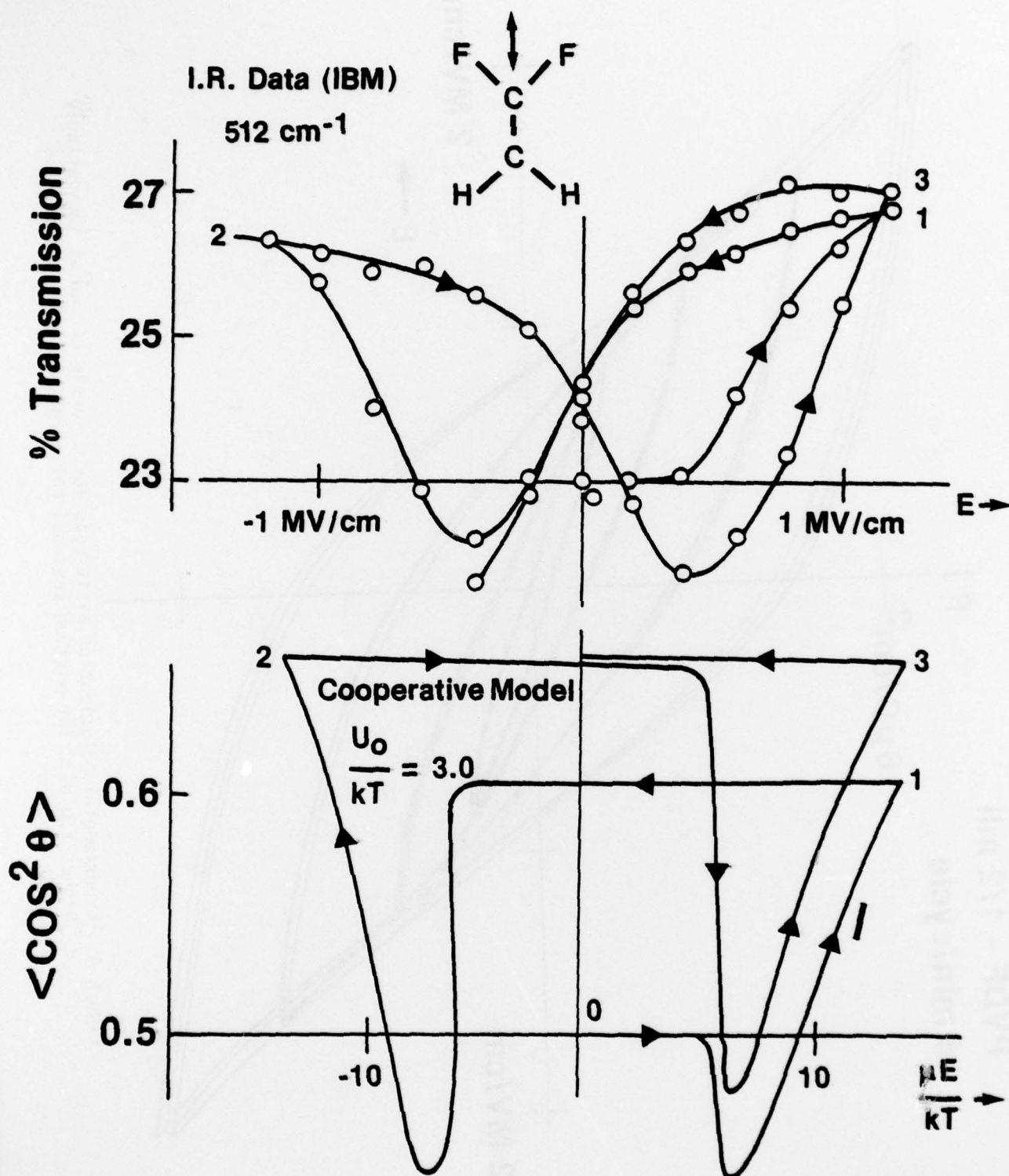


Figure 5. Experimental (Reference 3) and calculated infra red transmission hysteresis for a vibrational polarized along the CF<sub>2</sub> dipole in the  $\beta$  crystal phase.

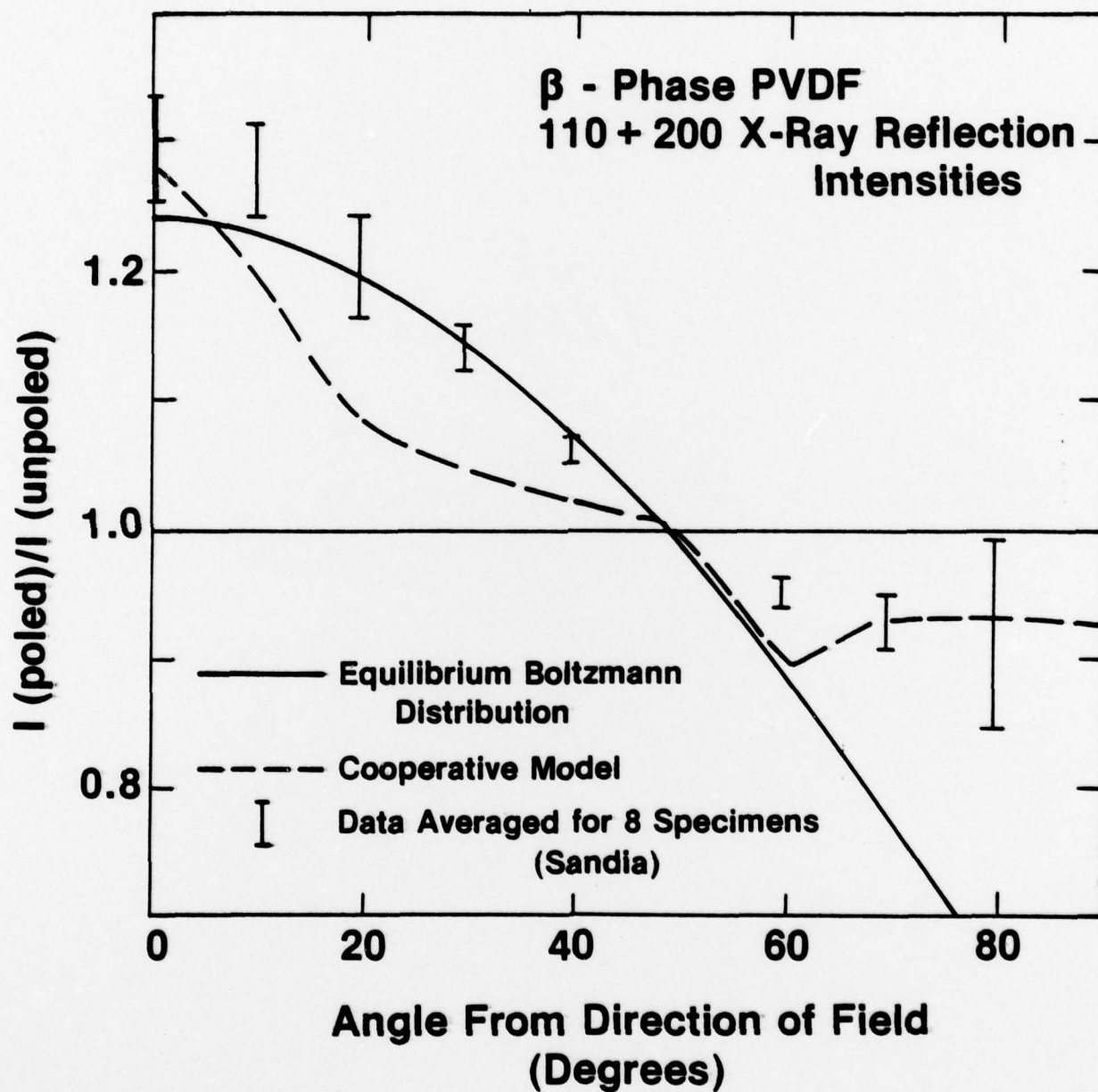


Figure 6. X-ray pole figure data from Reference 5 (error bars) and calculated results from the 6-site ferroelectric model (dashed lines) and an equilibrium distribution (solid line).

TECHNICAL REPORT DISTRIBUTION LIST, GEN

	<u>No.</u> <u>Copies</u>		<u>No.</u> <u>Copies</u>
Office of Naval Research 800 North Quincy Street Arlington, Virginia 22217 Attn: Code 472	2	Defense Documentation Center Building 5, Cameron Station Alexandria, Virginia 22314	12
ONR Branch Office 536 S. Clark Street Chicago, Illinois 60605 Attn: Dr. George Sandoz	1	U.S. Army Research Office P.O. Box 1211 Research Triangle Park, N.C. 27709 Attn: CRD-AA-IP	1
ONR Branch Office 715 Broadway New York, New York 10003 Attn: Scientific Dept.	1	Naval Ocean Systems Center San Diego, California 92152 Attn: Mr. Joe McCartney	1
ONR Branch Office 1030 East Green Street Pasadena, California 91106 Attn: Dr. R. J. Marcus	1	Naval Weapons Center China Lake, California 93555 Attn: Dr. A. B. Amster Chemistry Division	1
ONR Area Office One Hallidie Plaza, Suite 601 San Francisco, California 94102 Attn: Dr. P. A. Miller	1	Naval Civil Engineering Laboratory Port Hueneme, California 93401 Attn: Dr. R. W. Drisko	1
ONR Branch Office Building 114, Section D 666 Summer Street Boston, Massachusetts 02210 Attn: Dr. L. H. Peebles	1	Professor K. E. Woehler Department of Physics & Chemistry Naval Postgraduate School Monterey, California 93940	1
Director, Naval Research Laboratory Washington, D.C. 20390 Attn: Code 6100	1	Dr. A. L. Slafkosky Scientific Advisor Commandant of the Marine Corps (Code RD-1) Washington, D.C. 20380	1
The Assistant Secretary of the Navy (R,E&S) Department of the Navy Room 4E736, Pentagon Washington, D.C. 20350	1	Office of Naval Research 800 N. Quincy Street Arlington, Virginia 22217 Attn: Dr. Richard S. Miller	1
Commander, Naval Air Systems Command Department of the Navy Washington, D.C. 20360 Attn: Code 310C (H. Rosenwasser)	1	Naval Ship Research and Development Center Annapolis, Maryland 21401 Attn: Dr. G. Bosmajian Applied Chemistry Division	1
		Naval Ocean Systems Center San Diego, California 91232 Attn: Dr. S. Yamamoto, Marine Sciences Division	1

Encl 1



TECHNICAL REPORT DISTRIBUTION LIST, 356A

	<u>No. Copies</u>		<u>No. Copies</u>
Dr. Stephen H. Carr Department of Materials Science Northwestern University Evanston, Illinois 60201	1	Picatinny Arsenal SMUPA-FR-M-D Dover, New Jersey 07801 Attn: A. M. Anzalone Building 3401	1
Dr. M. Broadhurst Bulk Properties Section National Bureau of Standards U.S. Department of Commerce Washington, D.C. 20234	2	Dr. J. K. Gillham Princeton University Department of Chemistry Princeton, New Jersey 08540	1
Dr. T. A. Litovitz Department of Physics Catholic University of America Washington, D.C. 20017	1	Douglas Aircraft Co. 3855 Lakewood Boulevard Long Beach, California 90846 Attn: Technical Library CI 290/36-84 AUTO-Sutton	1
Dr. R. V. Subramanian Washington State University Department of Materials Science Pullman, Washington 99163	1	Dr. E. Baer Department of Macromolecular Science Case Western Reserve University Cleveland, Ohio 44106	1
Dr. M. Shen Department of Chemical Engineering University of California Berkeley, California 94720	1	Dr. K. D. Pae Department of Mechanics and Materials Science Rutgers University New Brunswick, New Jersey 08903	1
Dr. V. Stannett Department of Chemical Engineering North Carolina State University Raleigh, North Carolina 27607	1	NASA-Lewis Research Center 21000 Brookpark Road Cleveland, Ohio 44135 Attn: Dr. T. T. Serofini, MS-49-1	1
Dr. D. R. Uhlmann Department of Metallurgy and Material Science Center for Materials Science and Engineering Massachusetts Institute of Technology Cambridge, Massachusetts 02139	1	Dr. Charles H. Sherman, Code TD 121 Naval Underwater Systems Center New London, Connecticut	1
Naval Surface Weapons Center White Oak Silver Spring, Maryland 20910 Attn: Dr. J. M. Augl Dr. B. Hartman	1	Dr. William Risen Department of Chemistry Brown University Providence, Rhode Island 02192	1
Dr. G. Goodman Globe Union Incorporated 5757 North Green Bay Avenue Milwaukee, Wisconsin 53201	1	Dr. Alan Gent Department of Physics University of Akron Akron, Ohio 44304	1



TECHNICAL REPORT DISTRIBUTION LIST, 356A

	<u>No.</u> <u>Copies</u>		<u>No.</u> <u>Copies</u>
Mr. Robert W. Jones Advanced Projects Manager Hughes Aircraft Company Mail Station D 132 Culver City, California 90230	1	Dr. T. J. Reinhart, Jr., Chief Composite and Fibrous Materials Branch Nonmetallic Materials Division Department of the Air Force Air Force Materials Laboratory (AFSC) Wright-Patterson Air Force Base, Ohio 4543	1
Dr. C. Giori IIT Research Institute 10 West 35 Street Chicago, Illinois 60616	1	Dr. J. Lando Department of Macromolecular Science Case Western Reserve University Cleveland, Ohio 44106	
Dr. M. Litt Department of Macromolecular Science Case Western Reserve University Cleveland, Ohio 44106	1	Dr. J. White Chemical and Metallurgical Engineering University of Tennessee Knoxville, Tennessee 37916	1
Dr. R. S. Roe Department of of Materials Science and Metallurgical Engineering University of Cincinnati Cincinnati, Ohio 45221	1	Dr. J. A. Manson Materials Research Center Lehigh University Bethlehem, Pennsylvania 18015	1
Dr. L. E. Smith U.S. Department of Commerce National Bureau of Standards Stability and Standards Washington, D.C. 20234	1	Dr. R. F. Helmreich Contract RD&E Dow Chemical Co. Midland, Michigan 48640	1
Dr. Robert E. Cohen Chemical Engineering Department Massachusetts Institute of Technology Cambridge, Massachusetts 02139	1	Dr. R. S. Porter University of Massachusetts Department of Polymer Science and Engineering Amherst, Massachusetts 01002	1
Dr. David Roylance Department of Materials Science and Engineering Massachusetts Institute of Technology Cambridge, Massachusetts 02039	1	Professor Garth Wilkes Department of Chemical Engineering Virginia Polytechnic Institute and State University Blacksburg, Virginia 24061	1
Dr. T. P. Conlon, Jr., Code 3622 Sandia Laboratories Sandia Corporation Albuquerque, New Mexico	1	Dr. Kurt Baum Fluorochem Inc. 6233 North Irwindale Avenue Azusa, California 91702	1
Dr. Martin Kaufmann, Head Materials Research Branch, Code 4542 Naval Weapons Center China Lake, California 93555	1	Professor C. S. Paik Sung Department of Materials Sciences and Engineering Massachusetts Institute of Technology Cambridge, Massachusetts 02139	1